HHS Public Access

Author manuscript

Cell Microbiol. Author manuscript; available in PMC 2016 December 01.

Published in final edited form as:

Cell Microbiol. 2015 December ; 17(12): 1868–1882. doi:10.1111/cmi.12478.

Plasmodium falciparum adhesion domains linked to severe malaria differ in blockade of endothelial protein C receptor

Sowmya Sampath[1,‡], **Andrew Jay Brazier**[1,‡], **Marion Avril**[1,‡], **Maria Bernabeu**[1], **Vladimir Vigdorovich**[1], **Anjali Mascarenhas**[2], **Edwin Gomes**[3], **D. Noah Sather**[1], **Charles T. Esmon**[4], and **Joseph D. Smith**[1,5,*]

[1]Center for Infectious Disease Research (formerly Seattle Biomedical Research Institute), Seattle, Washington, 98109, USA

[2]University of Washington, Department of Chemistry, Seattle, Washington, 98195, USA

[3]Goa Medical College & Hospital, Bambolim, Goa, India

[4]Coagulation Biology Laboratory, Oklahoma Medical Research Foundation, Oklahoma City, OK, 73104, USA

[5]Department of Global Health, University of Washington, Seattle, Washington, 98195, USA

Summary

Cytoadhesion of *Plasmodium falciparum*-infected erythrocytes to endothelial protein C receptor (EPCR) is associated with severe malaria. It has been postulated that parasite binding could exacerbate microvascular coagulation and endothelial dysfunction in cerebral malaria by impairing the protein C-EPCR interaction, but the extent of binding inhibition has not been fully determined. Here we expressed the cysteine rich interdomain region (CIDRα1) domain from a variety of DC8 and DC13 *P. falciparum* erythrocyte membrane 1 (PfEMP1) proteins and show they interact in a distinct manner with EPCR resulting in weak, moderate, and strong inhibition of the APC-EPCR interaction. Overall, there was a positive correlation between CIDRα1-EPCR binding activity and APC blockade activity. In addition, our analysis from a combination of mutagenesis and blocking antibodies finds that an Arg81 (R81) in EPCR plays a pivotal role in CIDRα1 binding, but domains with weak and strong APC blockade activity were distinguished by their sensitivity to inhibition by anti-EPCR mAb 1535, implying subtle differences in their binding footprints. These data reveal a previously unknown functional heterogeneity in the interaction between *P. falciparum* and EPCR and have major implications for understanding the distinct clinical pathologies of cerebral malaria and developing new treatment strategies.

Keywords

Plasmodium falciparum; malaria; antigenic variation; adhesion

*Corresponding author. Joseph D. Smith, Tel: 206-256-7384, Fax: 206-256-7229, joe.smith@cidresearch.org.
‡These authors contributed equally to this work.

Conflicts of Interest

The authors have no conflicts of interest to declare.

Introduction

Cerebral malaria (CM) is a life-threatening complication associated with the massive sequestration of *P. falciparum*-infected erythrocytes (IE) in the microvasculature of the brain (MacPherson *et al.*, 1985;Taylor *et al.*, 2004). Even with anti-malaria drug treatment and supportive care, about 10–15% of those who develop CM die (Beales *et al.*, 2000;Dondorp *et al.*, 2010) and many survivors have neurological complications (Birbeck *et al.*, 2010). A pediatric autopsy study in Malawi defined two different CM groups (Taylor *et al.*, 2004). CM1 is characterized by IE sequestration without intravascular pathology, while the defining characteristics of CM2 are IE sequestration plus ring hemorrhages, fibrin thrombi, and intravascular monocytes (Dorovini-Zis *et al.*, 2011;Milner, Jr. *et al.*, 2014). There is still limited understanding of the molecular mechanisms responsible for these pathophysiological differences. Consequently, there has been significant interest in characterizing the parasite-host receptor interactions that support cerebral sequestration.

IE binding is mediated by a large and clonally variant gene family called *var* genes or *P. falciparum* erythrocyte membrane protein 1 (PfEMP1) (Baruch *et al.*, 1995;Smith *et al.*, 1995;Su *et al.*, 1995). PfEMP1 contain multiple Duffy binding like (DBL) and cysteine-rich interdomain region (CIDR) adhesion domains, which are classified into different types (e.g. α, β, γ) and subtypes (e.g. α1.1–1.8) by sequence similarity (Rask *et al.*, 2010;Smith *et al.*, 2000). Recent evidence indicates that parasites expressing a specific combination of PfEMP1 adhesion domains, called domain cassettes (DC) 8 and 13 (Rask *et al.*, 2010) are increased in severe pediatric malaria infections (Bertin *et al.*, 2013;Lavstsen *et al.*, 2012) and bind human brain microvascular endothelial cells in vitro (Avril *et al.*, 2012;Avril *et al.*, 2013;Claessens *et al.*, 2012). Of interest, most PfEMP1 bind to CD36 (Robinson *et al.*, 2003), however, DC8 and DC13 PfEMP1 bind to endothelial protein C receptor (EPCR) via the CIDRα1.1/CIDRα1.4 domains instead (Turner *et al.*, 2013).

The finding that EPCR is a binding partner for *P. falciparum* has significant implications for CM disease mechanisms because it is a receptor for protein C, a plasma protein that plays a major role in controlling thrombosis and regulating endothelial cell apoptosis and barrier properties in response to inflammation and hypoxia (Esmon, 2003;Mosnier *et al.*, 2007). EPCR is structurally related to the major histocompatibility class 1/CD1 family of proteins (Oganesyan *et al.*, 2002). By binding to the carboxylation/gamma-carboxyglutamic (Gla-domain) in protein C, EPCR facilitates the production of activated protein C (APC) by the thrombin-thrombomodulin complex (Fukudome *et al.*, 1996;Mosnier *et al.*, 2007;Regan *et al.*, 1997;Stearns-Kurosawa *et al.*, 1996). There is significant cross-regulation and opposing activities between the APC-EPCR and thrombin pathways. Whereas APC is an anti-coagulant protease and elicits cytoprotective and barrier strengthening signals in endothelial cells, thrombin is a pro-coagulant protease that cleaves soluble fibrinogen to create fibrin clots and weakens endothelial barrier properties. In addition, APC-EPCR can modify thrombin signaling by various potential mechanisms reviewed in (Rao *et al.*, 2014). Notably, there is decreased EPCR staining and increased fibrin deposition at sites of IE sequestration in pediatric CM autopsies (Moxon *et al.*, 2013), suggesting parasite blockade of the APC-EPCR pathways may play a role in cerebral malaria pathogenesis. Indeed, new

CIDRα1.4:EPCR co-crystal structures show substantial overlap between CIDRα1.4 and APC binding interfaces (Lau *et al.*, 2015;Oganesyan *et al.*, 2002).

Although these findings indicate similarity between CIDRα1 and APC binding interfaces, few CIDRα1 domains have been analyzed for APC blockade activity (Turner *et al.*, 2013). In addition, EPCR co-crystal structures exist for only one type of parasite domain (Lau *et al.*, 2015). In this study, we show that DC8 and DC13 parasite domains linked to severe malaria differ in APC-blockade activity.

Results

CIDRα1 domains have different binding activity for EPCR

The CIDR domain in the PfEMP1 semi-conserved head structure has a key role in *P. falciparum* binding to the microvascular receptors CD36 and EPCR (Baruch *et al.*, 1997;Robinson *et al.*, 2003;Turner *et al.*, 2013). Sequence and binding analysis has distinguished CD36 binding domains (CIDRα2–6 subtypes) and EPCR binding domains (CIDRα1.1 and CIDRα1.4–1.8 subtypes) (Fig. 1A). Two co-crystal structures have been solved for CIDRα1.4-EPCR complexes (Lau *et al.*, 2015), but no co-crystals exist for other CIDRα1 subtypes. For this study, we compared the CIDRα1.1 sub-type found in DC8 PfEMP1 and the CIDRα1.4 sub-type found in DC13 PfEMP1 (Fig. 1A).

In total, seven CIDR recombinant proteins were expressed, including a negative control, CD36-binding domain (Var14CIDRα5), four DC8 domains (Var19CIDRα1.1, Var06CIDRα1.1, Var20CIDRα1.1, and 25-2-4CIDRα1.1 from an India patient isolate), and the two solved DC13 domains (Var07CIDRα1.4 and HB3Var03CIDRα1.4) (Fig. 1B). The recombinant proteins were designed with similar domain boundaries using the varDom server (http://genome.cbs.dtu.dk/services/VarDom/) (Rask *et al.*, 2010), except the Var19CIDRα1.1 construct had a slightly longer C-terminus (58 amino acids) to facilitate protein production (Table S1). Following a 2-step purification process using an amino-terminal His tag and a carboxy-terminal strepII tag, each of the purified proteins ran as a single dominant product in SDS-PAGE gels at their expected molecular weight and generated a single band when detected with an anti-strepII antibody (Fig. 1B).

To investigate the binding properties of recombinant CIDR domains, binding affinity and association constants were measured using bio-layer interferometry (BLI). For these experiments, recombinant EPCR was produced with a C-terminal biotinylation tag for coupling to a BLI sensor probe. As expected, the negative control, CD36 binding Var14CIDRα5 domain did not bind recombinant EPCR (Fig. 2A and Table S2). Consistent with previous kinetic measurements by surface plasmon resonance (Lau *et al.*, 2015;Turner *et al.*, 2013), the Var07CIDRα1.4 and HB3Var03CIDRα1.4 recombinant proteins had low nanomolar binding constants (Kd 1–3 nM) (Fig. 2A). By comparison, the DC8 CIDRα1.1 domains varied in affinity by more than 100-fold. Var20CIDRα1.1 had the strongest affinity of any of the CIDRα1domains mainly due to its extremely low off-rate, Var19CIDRα1.1 and 25-2-4CIDRα1.1 had intermediate binding affinity (Kd 10–40 nM) and Var06CIDRα1.1 had the weakest binding affinity of all domains tested (Kd 98 nM) (Fig. 2 and Table S2). Likewise, in a cell-based assay, all CIDRα1.1 and CIDRα1.4 domains

interacted in a specific and dose-dependent fashion with CHO-EPCR transfectants. However, Var19CIDRα1.1 and 25-2-4CIDRα1.1 domains had weaker binding activities and reached a lower saturation binding level than the other four CIDRα1 domains (Fig. 2B). In addition, Var06CIDRα1.1 had weak binding activity at low concentrations but achieved a higher binding level at high concentrations.

CIDRα1 domains diverge in APC blocking activity

To investigate binding competition between parasite domains and APC, we developed a binding assay with EPCR-transfected CHO745 cells (CHO745-EPCR). In this assay, CHO745-EPCR cells were co-incubated with a mixture of recombinant CIDR domains and APC, and binding was analyzed by flow cytometry. As a control, APC and recombinant CIDR domains bound specifically to CHO745-EPCR and not untransfected CHO-745 cells (Fig. S1). For the competition assay, CIDR domains were added at 50 or 250 μg/ml, which was generally equivalent to 70% or 100% saturation from the titration assay (Fig. 2B). In method 1, APC binding was detected with goat anti-APC antibodies. In the absence of CIDR domains, approximately 76% of CHO745-EPCR cells incubated with APC were labeled by anti-APC antibodies (mean fluorescence intensity (MFI) = 994) (Fig. 3A). In co-incubation assays, CIDR1α1 domains differed in APC blockade activity. Two DC8 CIDRα1.1 domains had limited or no APC inhibition (Var19CIDRα1.1 and 25-2-4CIDRα1.1), two DC8 CIDRα1.1 had moderate inhibition (Var06CIDRα1.1 and Var20CIDRα1.1), and consistent with their recent co-crystal structures (Lau *et al.*, 2015), both DC13 CIDRα1.4 domains strongly inhibited or abolished APC binding at both low and high concentrations. Low inhibitory domains had limited activity beyond the negative control CD36-binding Var14CIDRα5 domain and moderate inhibitory domains were only active at the higher 250 μg/ml concentration (Fig. 3A). Overall, there was a positive correlation between CIDRα1-EPCR binding affinity (Fig. 2) and APC blockade activity (Fig. 3), suggesting this may be a factor in APC inhibition activity. However, Var20CIDRα1.1 has the highest binding affinity for recombinant EPCR and moderate inhibitory activity, suggesting this is not the only determinant.

In method 2, APC was labeled at its active site with fluoroscein (Fl-APC) to facilitate detection of co-labeled cells. On its own, the percentage of cells that bound 50 μg/ml Fl-APC was 78% (MFI = 1329) (Fig. 3B). As expected, the negative control, CD36-binding Var14CIDRα5 bound poorly to CHO-EPCR cells (red dot plots, Fig. 3B) and the intensity of Fl-APC labeling was only slightly reduced after co-incubation with either 50 μg/ml (MFI 1127, purple dot plots) or 250 μg/ml (MFI 931, blue dot plots) of Var14CIDRα5 (Fig. 3B). By comparison, the three EPCR-binding CIDRα1 domains had strong binding activity for CHO-EPCR cells (red dot plots, Fig. 3B) and co-incubation with Fl-APC led to the appearance of doubly-labeled cell populations (blue and purple dot plots, Fig. 3B). Similar to method 1, there was a range of inhibition with CIDRα1.1 domains. At the higher concentration of recombinant CIDR, the proportion of double positive cells (DP) and MFI for APC was respectively: Var19CIDRα1.1 (DP 69%, MFI 746), Var06CIDRα1.1 (DP 62%, MFI 429), and Var07CIDRα1.4 (DP 28%, MFI 385) compared to the negative control, CD36 binding Var14CIDRα5 (DP <1%, MFI 931) (Fig. 3B). Therefore, the more inhibitory CIDR domains resulted in fewer DP cells and lower MFI for APC (multiplying DP% × MFI

of APC gives Var19CIDRα1.1 = 51,474, Var06CIDRα1.1 = 26,598, Var07CIDRα1.4 = 10,780). Taken together, these findings suggest that DC8 CIDRα1.1 and DC13 CIDRα1.4 both bind in close proximity to APC, as supported by the CIDRα1.4-EPCR co-crystal (Lau *et al.*, 2015). However, some CIDR may occlude the APC binding site more than others.

R81 in EPCR plays a pivotal role in the binding interaction of both weak and strongly inhibitory CIDRα1 domains

An EPCR co-crystal has been solved with the strongly inhibitory Var07CIDRα1.4 and HB3var03CIDRα1.4 domains (Lau *et al.*, 2015). However, nothing is known about the fine specificity of the EPCR interaction with DC8 CIDRα1.1 subtype domains. To investigate if weak and strongly inhibitory CIDR domains engage different EPCR surfaces, we next investigated if any residues previously identified as important for APC binding may also contribute to parasite adhesion. Binding of protein C/APC has been shown to be mediated almost entirely by the vitamin K-dependent Gla-domain (Regan *et al.*, 1997). A co-crystal between the Gla-domain of APC and EPCR has identified contact residues (Oganesyan *et al.*, 2002) and ten residues distributed across the α1–α2 helices have been implicated in APC binding with the aid of site directed mutagenesis (Liaw *et al.*, 2001). For this study, eight of these residues were generated as point mutants in stably transfected CHO-745 cells (Fig. 4A). In addition, three other single point mutants (Q134A, D136A, or S141A) were made on the backside of the α2 helix at an adjacent region to the APC binding site (Fig. 4A). To ensure relatively equivalent cell surface levels, CHO745-EPCR mutants were sorted for surface expression by flow cytometry using anti-EPCR mAb 1500 because its epitope has been fine mapped and is not affected by any of these mutations (Liaw *et al.*, 2001). To normalize EPCR surface levels between wild-type and EPCR mutants, flow sorted cell populations were analyzed by anti-EPCR mAbs 252 and 1500. Relative to wild type EPCR, all mutants were expressed within two fold difference (Fig. 4B). Furthermore, all EPCR mutants were nearly equally recognized by mAbs 1500 and 252, with the exception of R81A and R87A. These two mutants had diminished recognition by mAb 252 compared to mAb 1500 (Fig. 4B, antibody ratios). From this, we conclude the EPCR mutants contained proper conformational epitopes and that blocking antibody mAb 252 may bind near residues R81 and R87.

Next, EPCR mutants were analyzed with Fl-APC. From crystallographic analysis, residue E86 of EPCR is critical for APC binding, residue R87 makes a hydrogen bond, and residues Y154 and T157 participate in hydrophobic interactions (Oganesyan *et al.*, 2002). Consistent with previous results (Liaw *et al.*, 2001), binding of APC to E86 variant is severely affected (>98% loss). Similarly, mutants of other APC contact residues (R87, F146, and Y154) are profoundly compromised in APC binding (greater than 80% loss), and residues in the middle of the α2 helix (T157, R158 and E160) or R81A, which did not directly contact APC in the co-crystal structure (Oganesyan *et al.*, 2002), are moderately affected (40–60% loss) (Fig. 4C). As expected, none of the three control mutants on the backside of the α2 helix (Q134A, D136A, or S141A) had an effect on APC binding.

In contrast, R81A was the only mutation that reduced binding of both Var19CIDRα1.1 and Var07CIDRα1.4 recombinant proteins (90% and 80% decrease, respectively) and IT4var19

and IT4var07-expressing IE (50% and 40% decrease, respectively) (Fig. 5A–B). In addition, the E86A mutation had a modest reduction in IT4var19 parasite binding (~30%) and IT4var07 parasite binding (~40%) compared to the nearly complete loss of APC binding (compare Figs. 4B and 5). However, the E86A mutant led to no reduction in binding of the matching CIDR recombinant proteins.

These findings are consistent with CIDRα1.4-EPCR co-crystals (Lau *et al.*, 2015) showing R81 in EPCR contacts a semi-conserved glutamine (Q) residue in Var07CIDRα1.4 and HB3Var03CIDRα1.4 (Fig. 5C), but neither domain directly contacts E86 in EPCR. Furthermore, point mutation of the Q657 residue in HB3Var03CIDRα1.4 reduces EPCR binding activity by 200-fold (Lau *et al.*, 2015), supporting the importance of the R81-Q657 interaction. Our analysis suggests that both weak and strongly inhibitory CIDRα1 domains interact with the R81 residue in EPCR via the Q/E residue in CIDRα1 domains (Fig. 5C). Based on the recent CIDRα1.4-EPCR co-crystal (Lau *et al.*, 2015), this arrangement would also position them to insert an adjacent conserved phenylalanine residue into the EPCR groove (Fig. 5C).

Cross-inhibition between DC8 and DC13 CIDR domains

To further investigate the binding overlap between DC8 and DC13 CIDR domains, cross-inhibition studies were performed with IT4var19 (DC8) or IT4var07 (DC13) parasite lines. This analysis showed that recombinant DC8 and DC13 CIDR domains could inhibit binding of both types of parasites to transformed human brain endothelial cells (THBMEC) (Stins *et al.*, 2001) (Fig. 6A) and to CHOK1-EPCR cells (Fig. 6B). As expected, recombinant CIDRα1 domains with low EPCR binding activity (Var19CIDRα1.1 and Var06CIDRα1.1) had weaker parasite inhibitory activity than those with higher binding phenotypes (Var20CIDRα1.1 and the two DC13 CIDRα1.4 domains) (Fig. 6). In addition, the two parasite lines were cross-inhibited by both types of CIDR domains (Fig. 6), suggesting CIDRα1.1 and CIDRα1.4 domains have at least partially overlapping EPCR binding interfaces, despite differences in APC blockade activity.

Differential inhibition of CIDRα1 domains by anti-EPCR monoclonal antibodies

As another approach to investigate the interaction of weak and strongly inhibitory CIDRα1 domains, we employed monoclonal antibodies (mAbs) to EPCR that were previously used to characterize the binding interface of APC-EPCR (Liaw *et al.*, 2001). For these experiments, CHOK1 cells stably transfected with EPCR (CHOK1-EPCR) (Ghosh *et al.*, 2007) were used. In agreement with published findings (Liaw *et al.*, 2001), there was approximately a 56% loss of APC binding with mAb 252, a 75% loss with mAb 1535, and non-blocking mAb 1500 had no effect on APC binding (Fig. 7). Likewise, all CIDRα1 domains were partially inhibited by APC blocking mAbs 252 and 1535, but mAb 1500 had limited or no effect on most domains except for 25-2-4CIDRα1.1 (~60% reduction). Notably, Var19CIDRα1.1 and 25-2-4CIDRα1.1 were markedly more sensitive to inhibition by mAb1535 than other CIDRα1 domains (Fig. 7A).

To extend these observations, antibody inhibition studies were performed with IT4var19 (DC8) or IT4var07 (DC13) parasite lines on CHOK1-EPCR cells and transformed human

brain endothelial cells (THBMEC) (Stins *et al.*, 2001). Similar to recombinant CIDR domains, both parasite lines were inhibited by mAbs 252 and 1535, and were less sensitive to inhibition by mAb1500. Furthermore, as with the recombinant CIDR domains, mAb 1535 had weaker blocking activity for the IT4var07 parasite line than the IT4var19 parasite line (Fig. 7B).

Of interest, there was an inverse correlation between the APC blocking activity and anti-EPCR antibody sensitivity of CIDRα1 domains. In particular, mAb 1535 had much higher inhibitory activity on the two CIDR domains with weak APC blocking activity (Var19CIDRα1.1 and 25-2-4CIDRα1.1) than the other CIDR domains (Fig. 7C). The epitope for mAb 1535 has been localized to a part of the β sheet, the connecting loop and the first turn of the α2-helix (Fig. 7C), while the less inhibitory mAb 1500 targets a loop between the last two strands of the β-sheet within the region recognized by mAb 1535 (Fig. 7C) (Liaw *et al.*, 2001). Taken together, these findings indicate there is significant overlap in the binding interfaces of CIDRα1 domains irrespective of their capacity to block the APC-EPCR interaction. However, the differential blocking effect exhibited by mAb 1535 may provide molecular insight into how CIDRα1 domains are situated on EPCR relative to the APC binding site or mAb 1535 epitope.

Discussion

Recent evidence suggests that severe malaria isolates bind EPCR and may contribute to endothelial barrier dysfunction and coagulation defects in cerebral malaria by competing with APC binding to EPCR (Turner *et al.*, 2013). This hypothesis is supported by structural investigations showing considerable overlap between the CIDRα1.4 and APC binding sites on EPCR (Lau *et al.*, 2015;Oganesyan *et al.*, 2002), which suggests that EPCR-binding parasites block the protein C-EPCR interaction. In this study, we investigated the adhesion domains from two PfEMP1 subfamilies that have been linked to severe malaria and cerebral binding (Avril et al., 2013; Bertin et al., 2013; Claessens et al., 2012; Lavstsen et al., 2012). We show that parasite adhesion domains differ in APC blockade activity.

Prior to this study, the majority of CIDR-EPCR binding characterizations have been performed with recombinant EPCR and few CIDRα1 subtypes have been analyzed. We found that four DC8 CIDRα1.1 domains had low or moderate APC inhibitory activity. In contrast, two DC13 CIDRα1.4 had high inhibition activity, as predicted from their co-crystal structures with EPCR (Lau *et al.*, 2015). Despite 100-fold differences in EPCR binding affinity, CIDRα1 functional differences were not fully predicted by their binding kinetics to recombinant EPCR. Indeed, the Var20 CIDRα1.1 had the highest affinity of any of the tested domains, but exhibited intermediate APC blockade activity. Our analysis suggests there are inherent differences in the CIDRα1-EPCR interaction, which may in turn have important functional consequences on the extent of APC blockade.

To understand these phenotypic differences, a combination of EPCR mutagenesis, antibody blocking, and competition binding studies were performed. Our analysis showed that DC8 and DC13-expressing parasite lines were cross-inhibited by CIDRα1.1 and CIDRα1.4 domains, suggesting both adhesion types have at least partially overlapping binding surfaces

on EPCR. In addition, domains with low or high APC blockade activity recognize the R81 residue in EPCR, but were differentially sensitive to inhibition by anti-EPCR mAb 1535. From crystallographic analysis EPCR R81 contacts a semi-conserved glutamine residue in CIDRα1.4 (Lau *et al.*, 2015). Notably, the glutamine is part of an "FQ/E" motif that is highly conserved in DC8 and DC13 CIDRα1 domains (Fig. S2), even amongst CIDR domains that differ in their capacity to block the APC-EPCR interaction. The phenylalanine residue in this motif inserts into the hydrophobic groove of EPCR in the same location as the F4 residue of APC (Lau *et al.*, 2015). These findings suggest that CIDRα1.4 and CIDRα1.1 domains likely use the FQ/E motif to engage similar contact interfaces in EPCR, but low and high inhibitory domains may not engage EPCR in precisely the same fashion.

This possibility is supported by a negative correlation between APC blockade and mAb1535 blockade activity of CIDR domains. Whereas APC and CIDRα1.4 domains primarily contact the α1 helix and binding groove in EPCR (Lau *et al.*, 2015;Oganesyan *et al.*, 2002), the 1535 epitope has been partially mapped to the α2 helix in EPCR (Liaw *et al.*, 2001). Thus, this antibody may give some molecular insight into how different CIDRα1 domains are situated on EPCR, which may be related to the extent to which they occlude the APC or 1535 binding sites. While further work is needed to understand the precise structural details of these differential interactions, CIDRα1 domains include a number of variable loops and surprisingly only have limited conservation of EPCR contact residues (Lau *et al.*, 2015). It is possible that CIDR sequence polymorphism could also influence their precise angle of engagement, the specific contact interface, and the space they occupy on EPCR.

The functional divergence in APC blockade activity has important implications for pathogenic mechanisms in cerebral malaria. Brain microvascular cells lack thrombomodulin expression (Ishii *et al.*, 1986;Moxon *et al.*, 2013) and therefore have limited capacity to generate APC in situ. Consequently, the brain may be more dependent on systematically released APC in the blood circulation and especially vulnerable to parasite blockade of the APC-EPCR interaction. Indeed, the companion manuscript from Gillrie *et al.* found that representative DC8 CIDRα1.1 and DC13 CIDRα1.4 domains differed in the ability to block APC generation and APC binding to primary endothelial cells, as well as to modulate thrombin-induced barrier dysfunction of endothelial cells, consistent with our findings here. Notably, in malaria autopsy studies, UpsB *var* transcripts were increased in cerebral vessels from CM1 cases and UpsA transcripts in CM2 cases (Tembo *et al.*, 2014). The UpsB promoter is associated with CD36 binding parasites and the chimeric DC8 *var* gene (UpsB promoter and group A coding region), neither of which would be expected to have as potent APC blockade activity as the UpsA associated DC13 CIDRα1.4 domain. Thus, it is interesting to speculate that differences in the proportions of strongly APC blocking parasite binding variants may be a factor in the pathophysiological distinction between CM1/CM2 cases. Future studies will be needed to determine how variability in the CIDRα1-EPCR interaction influences disease severity.

Experimental procedures

Parasite culture

P. falciparum parasites were cultured under standard conditions using human O red blood cells in RPMI-1640 medium (Invitrogen) supplemented with 10% pooled human A+ serum. Parasite lines expressing either IT4var19 (DC8) or IT4var7 (DC13) were cloned by limiting dilution after selection on human brain (Avril *et al.*, 2012) or lung endothelial cells (Avril *et al.*, 2013), respectively. Parasites lines were routinely synchronized by treatment with 5% sorbitol and gelatin flotation assays were performed to ensure IEs maintained their "knob-like" adhesion complexes. To ensure IT4var19 and IT4var07 parasite lines maintained a single dominant *var* transcript, multiple parasite cryopreserves were made after limiting dilution cloning. Prior to freezing, RNA was collected and the dominant expression of a single *var* transcript was determined using gene-specific *var* primers as described previously (Janes *et al.*, 2011). Parasite cultures were typically maintained for less than 30–40 cycles and RNA was periodically collected and analyzed for *var* transcription. If the dominant *var* transcript became reduced below 70% of the total *var* transcripts, the parasite line was replaced with an earlier freeze.

Recombinant CIDR domains

Recombinant CIDR domains were produced as His_6-MBP-TEV-PfEMP1 insert-StrepII-tagged proteins in pSHuffle Express (NEB) expression hosts as previously described (Avril *et al.*, 2013). CIDR constructs were designed with similar domain boundaries using the varDom server (http://genome.cbs.dtu.dk/services/VarDom/) (Rask *et al.*, 2010). The 25-2-4CIDRα1.1 domain was amplified from blood collected from an India patient using primers that target the flanking DBLα2 domain (5' GYTCARAWTATTGCCAACCC) and DBLβ12 domain (5' TAATCTTCTATKGGGATACCATTACA) in the DC8 cassette (Lavstsen *et al.*, 2012). The sequences of recombinant proteins used in this study are provided in Table S1. Recombinant proteins were purified in a 2-step process using an amino-terminal His tag and a carboxy-terminal strepII tag. Purified proteins were analyzed by SDS-PAGE gels using GelCode Blue Protein Stain (Life Technologies) or Western analysis using a rabbit anti-StrepII primary antibody (A00626, Genscript) and goat anti-rabbit secondary antibody (SC-2054, Santa Cruz Biotechnology) following standard procedures. Purified proteins were stored at −80°C.

Antibody inhibition assay with recombinant CIDR domains and CHOK1-EPCR

For inhibition assays, stably transfected CHOK1-EPCR cells (Ghosh *et al.*, 2007) (kind gift of Dr. LVM Rao) were lifted with 1× PBS (10 mM EDTA). Prior to the binding assay, cells were washed and resuspended in complete HBSS (HBSS with 3 mM $CaCl_2$, 0.6 mM $MgCl_2$, 1% bovine serum albumin) to restore divalent cations (Liaw *et al.*, 2001). For each assay, 1×10^5 CHOK1-EPCR cells were pre-incubated for 30 min with rat anti-EPCR mAb (RCR-252, 50 μg/ml, Sigma) or mouse anti-EPCR mAbs 1500 or 1535 (both IgG1k, 0.2 μM) (Liaw *et al.*, 2001). Washed cells were then incubated with APC (P2200, 25 μg/ml, Sigma) or CIDRα1 recombinant proteins (50 μg/ml) in complete HBSS for 30 min. APC binding was detected with goat anti-human Protein C antibody (GAPC-AP, 20 μg/ml, Affinity Biologicals) followed by chicken anti-goat Alexa488 coupled antibody (A-21467,

10 μg/ml, Molecular Probes). Binding of CIDR recombinant proteins was assessed by labeling with rabbit polyclonal anti-StrepII tag antibody (10 μg/ml, A00626, Genscript) followed by goat anti-rabbit Alexa488 coupled antibodies (A-11070, 4 μg/ml, Molecular Probes). Control samples were labeled with secondary antibodies alone to set gates. Labelled cells were analyzed by LSRII (Becton Dickinson). Data was analyzed by FlowJO 10 software (Tree Star Inc.).

BLI analysis of CIDR-EPCR binding

Binding kinetic analysis of the CIDR-EPCR interaction was performed on the Octet QKe instrument (ForteBio, Inc). The EPCR recombinant protein was produced as a secreted soluble protein in HEK293F cells as previously described (Carbonetti *et al.*, 2014;Harupa *et al.*, 2014) with slight modifications. Briefly, a modified, codon optimized EPCR sequence was cloned into the mammalian cell vector pCEP4 (Life Technologies, Grand Island, NY) for transient expression in mammalian cell cultures. The insert contained the extracellular region of EPCR (residues 18–210) and included an AviTag™ peptide sequence at the C-terminus for targeted biotinylation, followed by a stop codon. Secreted recombinant protein was produced in HEK293F mammalian cells by high density transfection (12 μg/ml DNA added to 20 million cells/ml) using PEI Max (Polysciences) as a transfection reagent, as previously described (Sellhorn *et al.*, 2009). EPCR was captured from the culture supernatant with NiNTA resin and then purified by size exclusion chromatography. Purified monomeric EPCR was biotinylated in vitro using recombinant BirA ligase and subsequently purified by gel filtration. Biotinylated EPCR (50 μg/mL in PBS) was coupled to a streptavidin biosensor (ForteBio) for 3.3 min. The baseline signal was then recorded for 60 sec in kinetics buffer (PBS + 0.02% Tween-20, 100 μg/mL BSA, 0.005% sodium azide). For the association phase, binding was measured by immersion of the sensors into wells containing CIDR domains diluted in kinetics buffer for 600 s or 900 s. For the disassociation phase, sensors were then immersed in kinetics buffer for the indicated times. Mean k_{on} and k_{off} and apparent Kd values were determined from double-reference-subtracted data from 3 CIDR concentrations that were fitted globally to a 1:1 Langmuir binding model using the Data analysis software (ForteBio) and the concentration of CIDR domains.

EPCR Site-Directed mutagenesis

EPCR in pCMV6 expression vector (Origene) was used for generating EPCR mutants. Mutagenesis was performed with the QuikChange Lightning Site-Directed Mutagenesis Kit (Agilent) using the primers in Table S3. Wild-type (WT) and mutant EPCR sequences were confirmed by DNA sequencing.

Generation of EPCR Transfectants

CHO745 cells were transfected using GeneJuice transfection reagent (Novagen) according to the manufacturer's instruction. Transfected cells were selected with 1 mg/ml Geneticin (G418 Corning) and maintained on 0.25 mg/ml Geneticin. Stably transfected CHO745-EPCR cells (mutant and WT) were sorted by flow cytometry for EPCR surface expression using anti-EPCR mAb 1500.

Flow cytometric analysis of EPCR surface levels on transfected cell lines

Stably transfected CHO745-EPCR cells were lifted with 10 mM EDTA and washed with PBS. 1×10^5 cells were labeled with 0.2 μM of mouse anti-EPCR mAb 1535 (Liaw *et al.*, 2001) or with 20 μg/ml rat anti-EPCR mAb RCR-252. Binding of mouse and rat anti-EPCR mAbs was detected with goat anti-mouse Alexa488 coupled antibody or goat anti-rat Alexa488 coupled antibody (Molecular Probes). Antibody-labeled cells were analyzed by LSRII (Becton Dickinson) and data was analyzed by FlowJO 10 software (Tree Star Inc.). EPCR surface expression levels were normalized between wild-type and mutant EPCR by comparing anti-EPCR antibody reactivity on mutant EPCR cells relative to wild-type EPCR. The loss of antibody epitopes was analyzed by comparing the ratio of mAb252 and mAb1500 antibody reactivity on mutant EPCR cell line relative to wild-type EPCR cell line.

Generation of fluorescently labelled APC

Human APC (Hematologic Technologies) was labeled with PPACK-FITC (Molecular Innovations) at the active site according to manufacturer's protocol. The reaction was then extensively dialyzed to remove excess label. Fl-APC was stored at −80°C.

Competition binding assays between CIDR recombinant proteins and APC

For binding competition assays, CHO745-EPCR cells were lifted with 10 mM EDTA, washed, and 1×10^5 cells were co-incubated with 50 μg/ml APC and different concentrations of CIDR recombinant proteins for 30 min on ice. In parallel wells, cells were incubated with APC and CIDR recombinant proteins on their own. In method 1, unlabeled APC (Sigma) was used in the co-incubation. After two washes, binding of APC was detected with a goat anti-APC mAb (Affinity Biologicals) followed by a secondary Chicken anti-Goat antibody Alexa-488 (10 μg/ml, Molecular Probes, A-21467). In method 2, Fl-APC was used in the co-incubation. After two washes, co-labeling of CHO745-EPCR cells with Fl-APC and CIDR was analyzed. CIDR binding was detected with a rabbit anti-strepII antibody and goat anti-rabbit PE coupled antibodies (P2771MP, 2.5 μg/ml, Molecular Probes). Results were analyzed by flow cytometry, as described above.

Flow cytometric analysis of APC and CIDR domains binding to CHO745-EPCR mutants

The binding interactions of CHO745-EPCR (WT) or EPCR mutants was determined by incubating 1×10^5 cells with either 25 μg/ml of Fl-APC, Var19CIDRα1.1 (50 μg/ml) or Var07CIDRα1.4 (1 μg/ml) for 30 min. Cells were washed and binding of CIDR was detected with rabbit polyclonal anti-StrepII tag antibody (Genscript) followed by goat anti-rabbit Alexa488 coupled antibodies (Molecular Probes). Flow cytometry was done as described above. The binding levels were normalized by correcting for the surface expression levels of EPCR mutants compared to EPCR (WT) using anti-EPCR mAb 252 for normalization or mAb 1500 in the case of the R81 and R87 mutants.

Parasite assays

For IE binding assays to EPCR mutants, CHO745-EPCR (WT) or EPCR mutants were seeded on collagen coated 8 wells slides (BD Biocoat) 3 to 4 days before the assays and allowed to grow to confluency. Binding assays and washes were performed with pre-

warmed binding medium (RPMI-1640 medium containing 0.5% bovine serum albumin, pH 7.2). Gelatin-enriched IEs were resuspended to 5 $\times 10^6$ IEs/ml solution and then were added to a multiwell slide. After 1 h incubation at 37°C, non-binding erythrocytes were removed by inverting the slide in a slide washing chamber and allowing the non-binding cells to settle by gravity. For quantification, slides were fixed in 1% glutaraldehyde for 30 min at room temperature, then stained with 1× Giemsa for 5 min. Binding was quantified by determining the number of IEs adhering per mm^2 of endothelial cells in four random fields under 400× magnification.

For IE binding inhibition assays with antibodies or recombinant CIDR domains, CHOK1-EPCR or THBMEC cells (Avril *et al.*, 2012) were grown to a monolayer on 8 well slides. Cell monolayers were pre-incubated with rat anti-EPCR mAb (RCR-252, 50 μg/ml, Sigma) or mouse anti-EPCR mAbs 1500 or 1535 (0.2 μM), or 50 μg/ml CIDR domains for 30 minutes prior to addition of 5 $\times 10^6$ IEs/ml solution. IE binding assays were performed and quantified as described above.

Statistical analysis

Statistical analyses were performed using Prism software. Data were analyzed using Krustal-Wallis one-way Anova test or using a one-sample t test comparing the mean of test samples against a hypothetical mean of 100 (referring to the wild type or control value of 100%). P values: **** $p<0.0001$; *** $p<0.001$; ** $p<0.001$; * $p<0.05$; ns $p>0.05$.

Supplementary Material

Refer to Web version on PubMed Central for supplementary material.

Acknowledgement

We thank Dr. L. Vijaya Mohan Rao of The University of Texas Health Science Center at Tyler for providing the CHOK1-EPCR cell line. Funding for this work was provided by the National Institutes of Health (R56 AI104238, RO1 AI47953, and U19 AI089688).

References

Avril M, Brazier AJ, Melcher M, Sampath S, Smith JD. DC8 and DC13 var Genes Associated with Severe Malaria Bind Avidly to Diverse Endothelial Cells. PLoS Pathog. 2013; 9:e1003430. [PubMed: 23825944]

Avril M, Tripathi AK, Brazier AJ, Andisi C, Janes JH, Soma VL, Sullivan DJ Jr, Bull PC, Stins MF, Smith JD. A restricted subset of var genes mediates adherence of Plasmodium falciparum-infected erythrocytes to brain endothelial cells. Proc Natl Acad Sci U S A. 2012; 109:E1782–E1790. [PubMed: 22619321]

Baruch DI, Ma XC, Singh HB, Bi X, Pasloske BL, Howard RJ. Identification of a region of PfEMP1 that mediates adherence of Plasmodium falciparum infected erythrocytes to CD36: conserved function with variant sequence. Blood. 1997; 90:3766–3775. [PubMed: 9345064]

Baruch DI, Pasloske BL, Singh HB, Bi X, Ma XC, Feldman M, Taraschi TF, Howard RJ. Cloning the P. falciparum gene encoding PfEMP1, a malarial variant antigen and adherence receptor on the surface of parasitized human erythrocytes. Cell. 1995; 82:77–87. [PubMed: 7541722]

Beales PF, Brabin B, Dorman E, Gilles HM, Loutain L, Marsh K, Molyneux ME, Olliaro P, Schapira A, Touze J-E, Hien TT, Warrell DA, White N. Severe falciparum malaria. Trans R Soc Trop Med Hyg. 2000; 94(Suppl 1):S1–S90. [PubMed: 11103309]

Bertin GI, Lavstsen T, Guillonneau F, Doritchamou J, Wang CW, Jespersen JS, Ezimegnon S, Fievet N, Alao MJ, Lalya F, Massougbodji A, Ndam NT, Theander TG, Deloron P. Expression of the domain cassette 8 Plasmodium falciparum erythrocyte membrane protein 1 is associated with cerebral malaria in Benin. PLoS ONE. 2013; 8:e68368. [PubMed: 23922654]

Birbeck GL, Molyneux ME, Kaplan PW, Seydel KB, Chimalizeni YF, Kawaza K, Taylor TE. Blantyre Malaria Project Epilepsy Study (BMPES) of neurological outcomes in retinopathy-positive paediatric cerebral malaria survivors: a prospective cohort study. Lancet Neurol. 2010; 9:1173–1181. [PubMed: 21056005]

Carbonetti S, Oliver BG, Glenn J, Stamatatos L, Sather DN. Soluble HIV-1 envelope immunogens derived from an elite neutralizer elicit cross-reactive V1V2 antibodies and low potency neutralizing antibodies. PLoS ONE. 2014; 9:e86905. [PubMed: 24466285]

Claessens A, Adams Y, Ghumra A, Lindergard G, Buchan CC, Andisi C, Bull PC, Mok S, Gupta AP, Wang CW, Turner L, Arman M, Raza A, Bozdech Z, Rowe JA. A subset of group A-like var genes encodes the malaria parasite ligands for binding to human brain endothelial cells. Proc Natl Acad Sci U S A. 2012; 109:E1772–E1781. [PubMed: 22619330]

Dondorp AM, Fanello CI, Hendriksen IC, Gomes E, Seni A, Chhaganlal KD, Bojang K, Olaosebikan R, Anunobi N, Maitland K, Kivaya E, Agbenyega T, Nguah SB, Evans J, Gesase S, Kahabuka C, Mtove G, Nadjm B, Deen J, Mwanga-Amumpaire J, Nansumba M, Karema C, Umulisa N, Uwimana A, Mokuolu OA, Adedoyin OT, Johnson WB, Tshefu AK, Onyamboko MA, Sakulthaew T, Ngum WP, Silamut K, Stepniewska K, Woodrow CJ, Bethell D, Wills B, Oneko M, Peto TE, von SL, Day NP, White NJ. Artesunate versus quinine in the treatment of severe falciparum malaria in African children (AQUAMAT): an open-label, randomised trial. Lancet. 2010; 376:1647–1657. [PubMed: 21062666]

Dorovini-Zis K, Schmidt K, Huynh H, Fu W, Whitten RO, Milner D, Kamiza S, Molyneux M, Taylor TE. The neuropathology of fatal cerebral malaria in malawian children. Am J Pathol. 2011; 178:2146–2158. [PubMed: 21514429]

Esmon CT. The protein C pathway. Chest. 2003; 124:26S–32S. [PubMed: 12970121]

Fukudome K, Kurosawa S, Stearns-Kurosawa DJ, He X, Rezaie AR, Esmon CT. The endothelial cell protein C receptor. Cell surface expression and direct ligand binding by the soluble receptor. J Biol Chem. 1996; 271:17491–17498. [PubMed: 8663475]

Ghosh S, Pendurthi UR, Steinoe A, Esmon CT, Rao LV. Endothelial cell protein C receptor acts as a cellular receptor for factor VIIa on endothelium. J Biol Chem. 2007; 282:11849–11857. [PubMed: 17327234]

Harupa A, Sack BK, Lakshmanan V, Arang N, Douglass AN, Oliver BG, Stuart AB, Sather DN, Lindner SE, Hybiske K, Torii M, Kappe SH. SSP3 is a novel Plasmodium yoelii sporozoite surface protein with a role in gliding motility. Infect Immun. 2014; 82:4643–4653. [PubMed: 25156733]

Ishii H, Salem HH, Bell CE, Laposata EA, Majerus PW. Thrombomodulin, an endothelial anticoagulant protein, is absent from the human brain. Blood. 1986; 67:362–365. [PubMed: 3002524]

Janes JH, Wang CP, Levin-Edens E, Vigan-Womas I, Guillotte M, Melcher M, Mercereau-Puijalon O, Smith JD. Investigating the host binding signature on the Plasmodium falciparum PfEMP1 protein family. PLoS Pathog. 2011; 7:e1002032. [PubMed: 21573138]

Lau CK, Turner L, Jespersen JS, Lowe ED, Petersen B, Wang CW, Petersen JE, Lusingu J, Theander TG, Lavstsen T, Higgins MK. Structural conservation despite huge sequence diversity allows EPCR binding by the PfEMP1 family implicated in severe childhood malaria. Cell Host Microbe. 2015; 17:118–129. [PubMed: 25482433]

Lavstsen T, Turner L, Saguti F, Magistrado P, Rask TS, Jespersen JS, Wang CW, Berger SS, Baraka V, Marquard AM, Seguin-Orlando A, Willerslev E, Gilbert MT, Lusingu J, Theander TG. Plasmodium falciparum erythrocyte membrane protein 1 domain cassettes 8 and 13 are associated with severe malaria in children. Proc Natl Acad Sci U S A. 2012; 109:E1791–E1800. [PubMed: 22619319]

Liaw PC, Mather T, Oganesyan N, Ferrell GL, Esmon CT. Identification of the protein C/activated protein C binding sites on the endothelial cell protein C receptor. Implications for a novel mode of

ligand recognition by a major histocompatibility complex class 1-type receptor. J Biol Chem. 2001; 276:8364–8370. [PubMed: 11099506]

MacPherson GG, Warrell MJ, White NJ, Looareesuwan S, Warrell DA. Human cerebral malaria. A quantitative ultrastructural analysis of parasitized erythrocyte sequestration. Am J Pathol. 1985; 119:385–401. [PubMed: 3893148]

Milner DA Jr, Whitten RO, Kamiza S, Carr R, Liomba G, Dzamalala C, Seydel KB, Molyneux ME, Taylor TE. The systemic pathology of cerebral malaria in African children. Front Cell Infect Microbiol. 2014; 4:104. [PubMed: 25191643]

Mosnier LO, Zlokovic BV, Griffin JH. The cytoprotective protein C pathway. Blood. 2007; 109:3161–3172. [PubMed: 17110453]

Moxon CA, Wassmer SC, Milner DA Jr, Chisala NV, Taylor TE, Seydel KB, Molyneux ME, Faragher B, Esmon CT, Downey C, Toh CH, Craig AG, Heyderman RS. Loss of endothelial protein C receptors links coagulation and inflammation to parasite sequestration in cerebral malaria in African children. Blood. 2013; 122:842–851. [PubMed: 23741007]

Oganesyan V, Oganesyan N, Terzyan S, Qu D, Dauter Z, Esmon NL, Esmon CT. The crystal structure of the endothelial protein C receptor and a bound phospholipid. J Biol Chem. 2002; 277:24851–24854. [PubMed: 12034704]

Pongponratn E, Riganti M, Punpoowong B, Aikawa M. Microvascular sequestration of parasitized erythrocytes in human falciparum malaria: a pathological study. Am J Trop Med Hyg. 1991; 44:168–175. [PubMed: 2012260]

Rao LV, Esmon CT, Pendurthi UR. Endothelial cell protein C receptor: a multi-liganded and multi-functional receptor. Blood. 2014

Rask TS, Hansen DA, Theander TG, Gorm PA, Lavstsen T. Plasmodium falciparum Erythrocyte Membrane Protein 1 Diversity in Seven Genomes - Divide and Conquer. PLoS Comput Biol. 2010; 6:e1000933. [PubMed: 20862303]

Regan LM, Mollica JS, Rezaie AR, Esmon CT. The interaction between the endothelial cell protein C receptor and protein C is dictated by the gamma-carboxyglutamic acid domain of protein C. J Biol Chem. 1997; 272:26279–26284. [PubMed: 9334197]

Robinson BA, Welch TL, Smith JD. Widespread functional specialization of Plasmodium falciparum erythrocyte membrane protein 1 family members to bind CD36 analysed across a parasite genome. Mol Microbiol. 2003; 47:1265–1278. [PubMed: 12603733]

Sellhorn G, Caldwell Z, Mineart C, Stamatatos L. Improving the expression of recombinant soluble HIV Envelope glycoproteins using pseudo-stable transient transfection. Vaccine. 2009; 28:430–436. [PubMed: 19857451]

Smith JD, Chitnis CE, Craig AG, Roberts DJ, Hudson-Taylor DE, Peterson DS, Pinches R, Newbold CI, Miller LH. Switches in expression of Plasmodium falciparum var genes correlate with changes in antigenic and cytoadherent phenotypes of infected erythrocytes. Cell. 1995; 82:101–110. [PubMed: 7606775]

Smith JD, Subramanian G, Gamain B, Baruch DI, Miller LH. Classification of adhesive domains in the Plasmodium falciparum erythrocyte membrane protein 1 family. Mol Biochem Parasitol. 2000; 110:293–310. [PubMed: 11071284]

Stearns-Kurosawa DJ, Kurosawa S, Mollica JS, Ferrell GL, Esmon CT. The endothelial cell protein C receptor augments protein C activation by the thrombin-thrombomodulin complex. Proc Natl Acad Sci U S A. 1996; 93:10212–10216. [PubMed: 8816778]

Stins MF, Badger J, Sik KK. Bacterial invasion and transcytosis in transfected human brain microvascular endothelial cells. Microb Pathog. 2001; 30:19–28. [PubMed: 11162182]

Su XZ, Heatwole VM, Wertheimer SP, Guinet F, Herrfeldt JA, Peterson DS, Ravetch JA, Wellems TE. The large diverse gene family var encodes proteins involved in cytoadherence and antigenic variation of Plasmodium falciparum-infected erythrocytes. Cell. 1995; 82:89–100. [PubMed: 7606788]

Taylor TE, Fu WJ, Carr RA, Whitten RO, Mueller JS, Fosiko NG, Lewallen S, Liomba NG, Molyneux ME. Differentiating the pathologies of cerebral malaria by postmortem parasite counts. Nat Med. 2004; 10:143–145. [PubMed: 14745442]

Tembo DL, Nyoni B, Murikoli RV, Mukaka M, Milner DA, Berriman M, Rogerson SJ, Taylor TE, Molyneux ME, Mandala WL, Craig AG, Montgomery J. Differential PfEMP1 expression is associated with cerebral malaria pathology. PLoS Pathog. 2014; 10:e1004537. [PubMed: 25473835]

Turner L, Lavstsen T, Berger SS, Wang CW, Petersen JE, Avril M, Brazier AJ, Freeth J, Jespersen JS, Nielsen MA, Magistrado P, Lusingu J, Smith JD, Higgins MK, Theander TG. Severe malaria is associated with parasite binding to endothelial protein C receptor. Nature. 2013; 498:502–505. [PubMed: 23739325]

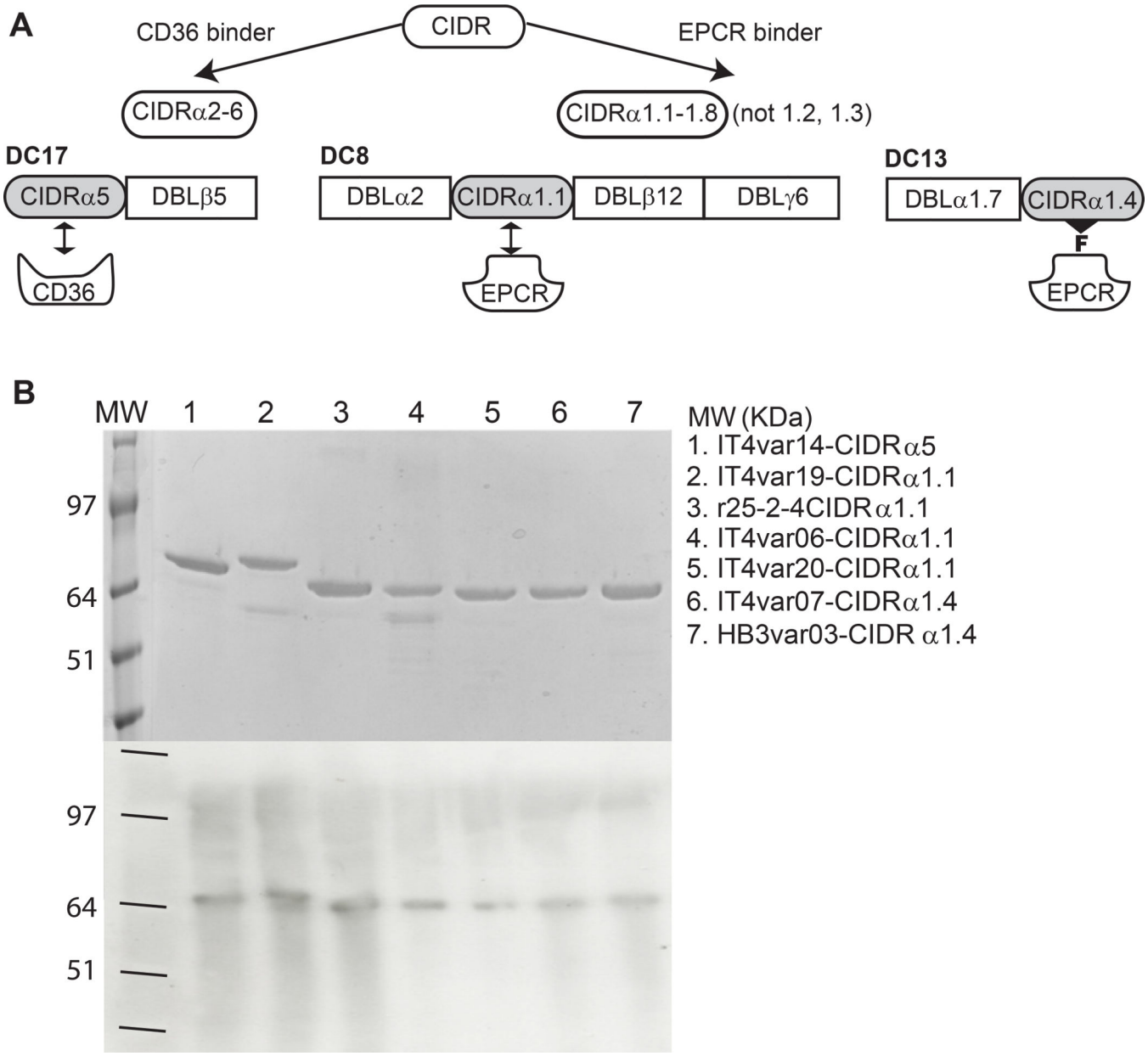

Fig. 1. Production of CIDR recombinant proteins

A. CIDR domains are categorized by sequence and binding criteria into CD36 binders (CIDRα2–6) and EPCR binders (CIDRα1.1 and 1.4–1.8). The schematics compare the domain architectures and types of CIDR domains found in DC17, DC8, and DC13 PfEMP1 forms analyzed in this study (Rask *et al.*, 2010). The CIDRα1.4 domain contains a phenylalanine residue that inserts into the EPCR binding groove (Lau *et al.*, 2015).

B. CIDR recombinant proteins were analyzed under non-reducing conditions in a SDS-PAGE gel and stained by GelCode Blue Protein Stain (top) or detected by immunoblot via anti-StrepII tag antibody (bottom).

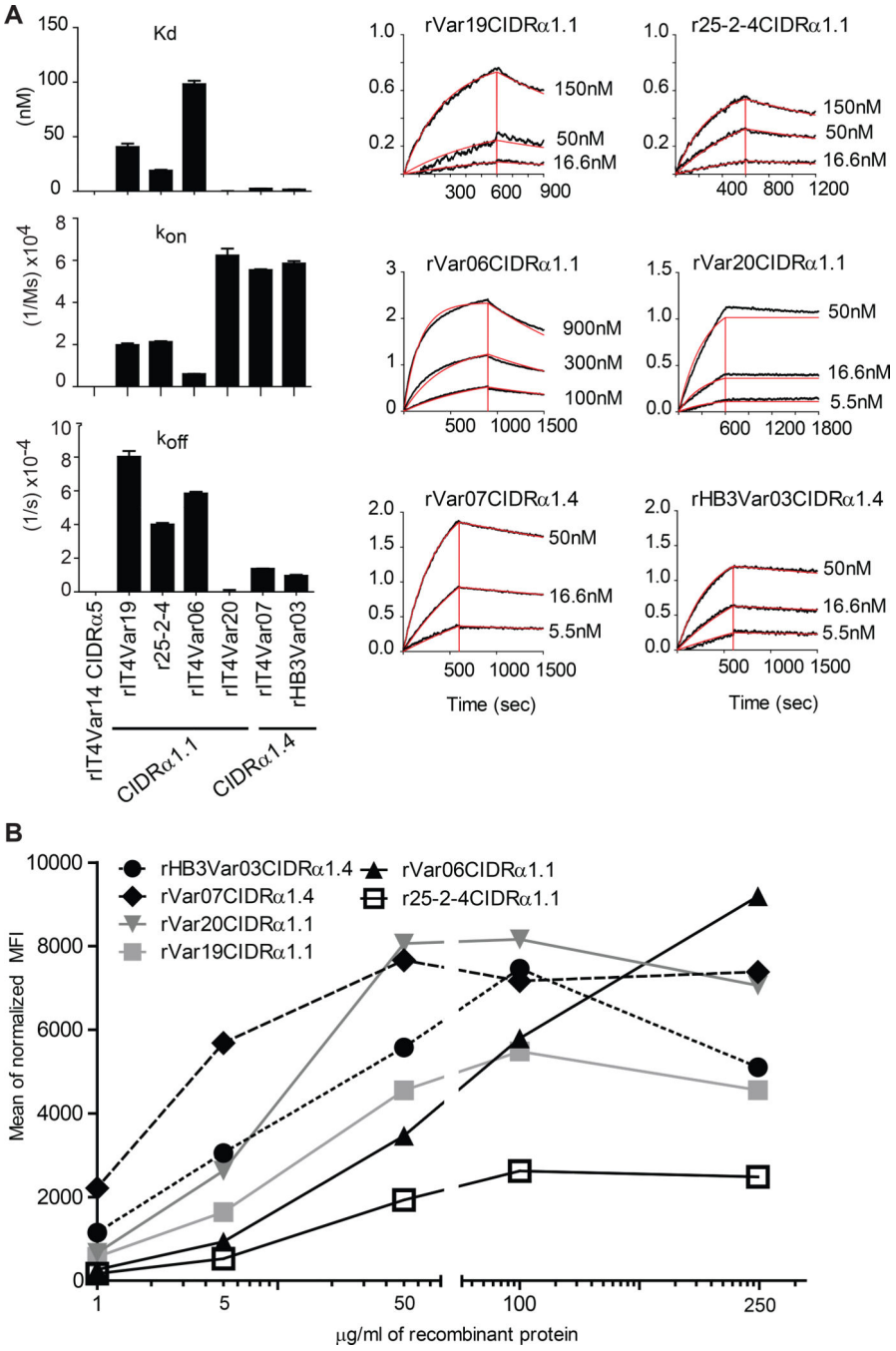

Fig. 2. CIDRα1 domains differ in EPCR binding activity

A. Binding kinetics between recombinant CIDR domains and recombinant soluble EPCR were quantified by BLI and summarized in bar graphs. Representative sensorgrams are shown for each CIDRα1 domain. Double referenced binding data are shown in black with corresponding kinetic fits to the data in red. A summary of binding kinetics is provided in Table S2.

B. Dose-dependent binding activity of CIDRα1 domains for CHO-EPCR cells analyzed by flow cytometry. Results are representative of two experiments.

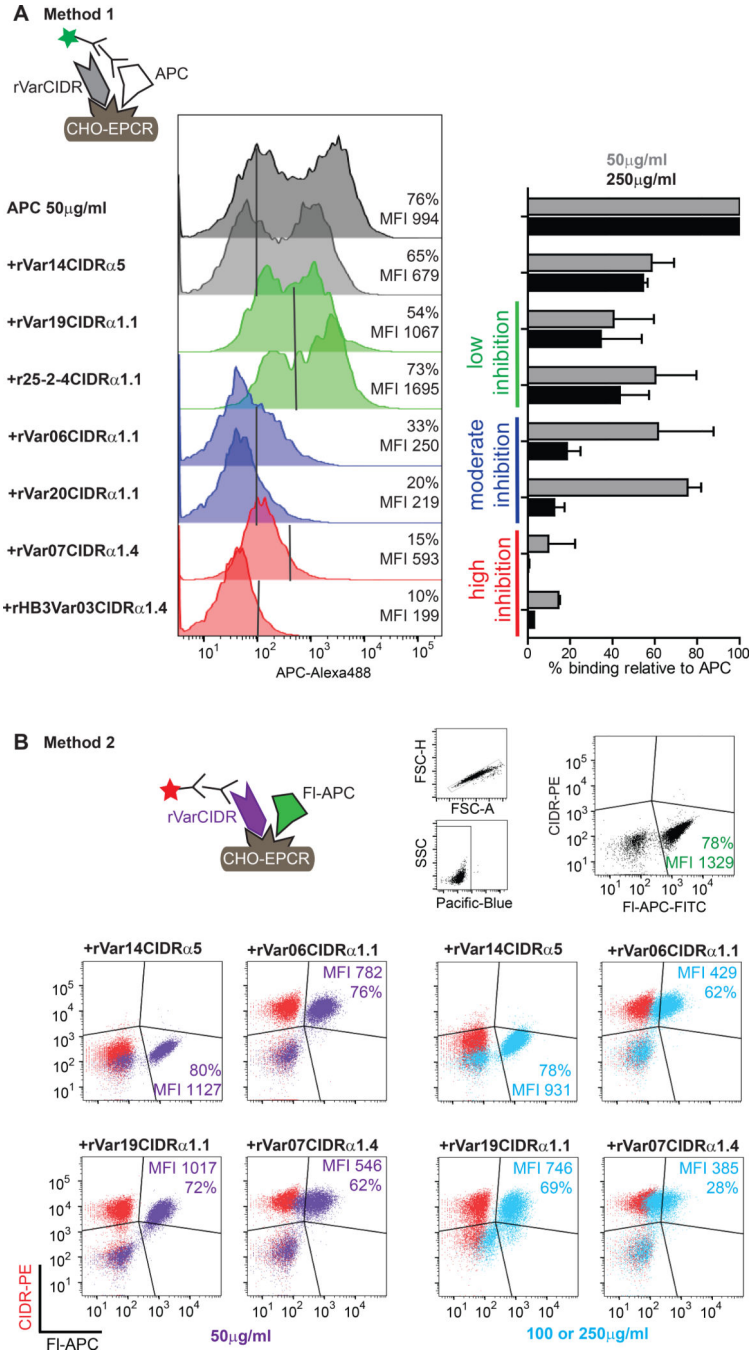

Fig. 3. CIDRα1 domains have divergent inhibitory activity for the APC-EPCR interaction

A. In method 1, CIDR recombinant proteins and APC (50 μg/ml) were co-incubated with CHO745-EPCR for 30 min and APC binding was detected by goat anti-APC antibodies. Histograms show APC binding in the presence or absence of 250 μg/ml CIDR domains. The recombinant CIDR domains were analyzed in two batches. The vertical line on each histogram shows control sample labeling of CHO-EPCR cells incubated with secondary antibodies alone on the specific day of analysis, which was used to set the gate for APC

positive cells. The percentage of APC binding at two CIDR concentrations is shown in the bar graphs (mean and error bars, n = 2 – 6 independent experiments).
B. In method 2, APC was specifically labeled at the active site with PPACK-FITC (Fl-APC) to facilitate detection of co-labeled cells. The gating strategy for live/dead cells and forward scatter is shown. The upper right panel shows CHO-EPCR cells incubated with 50 μg/ml Fl-APC alone (black dot plots). The other histograms show an overlay of CHO-EPCR cells incubated with CIDR recombinant proteins alone (red dot plots) or co-incubation of CIDR plus APC (purple dot plots, 50 μg/ml CIDR domain; blue dot plots, either 100 μg/ml Var07CIDRα1.4 or 250 μg/ml other CIDR domains). The percentage of single or double-labeled cells in each quadrant and the mean fluorescence intensity (MFI) of APC labeling are indicated. A cartoon illustration of the two detection methods is shown.

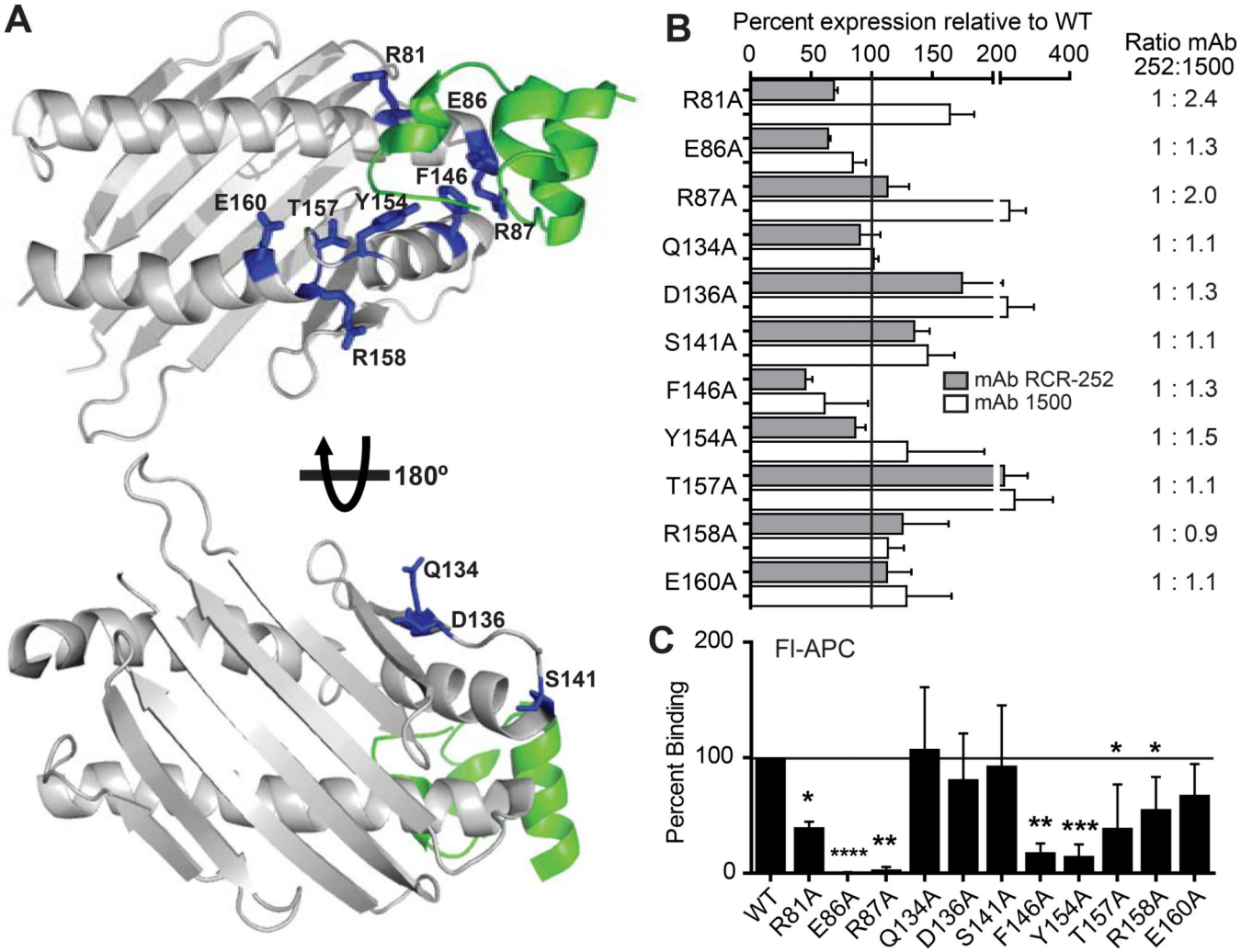

Fig. 4. Binding of APC to EPCR mutants

A. Ribbon schematic of EPCR (grey) – Gla-domain of APC (green) (PDB 1L8J) (Oganesyan *et al.*, 2002) with the 8 residues previously implicated in APC binding (Liaw *et al.*, 2001) shown as blue stick figures. Below is a reverse view of EPCR structure showing the location of 3 other residues mutated for this study.

B. CHO745-EPCR mutants were labeled with anti-EPCR mAbs 1500 and 252. The bar graphs compare the level of antibody recognition of mutant EPCR cells relative to wild type EPCR levels. The ratio of mAb252:1500 antibody recognition was analyzed for each mutant EPCR relative to wild-type EPCR to assess loss of antibody epitopes (mean and error bars, n = 2 – 6 independent experiments).

C. Binding of Fl-APC to EPCR mutants is shown relative to wild type EPCR. The percentage of APC binding is normalized for differences in surface expression levels of wild-type and mutant EPCR variants determined by mAbs 252 and 1500 (see methods). Data represent mean and error bars (n = 2 – 4 independent experiments), a one-sample t test was used to detect significance in binding between EPCR mutants and wild type EPCR.

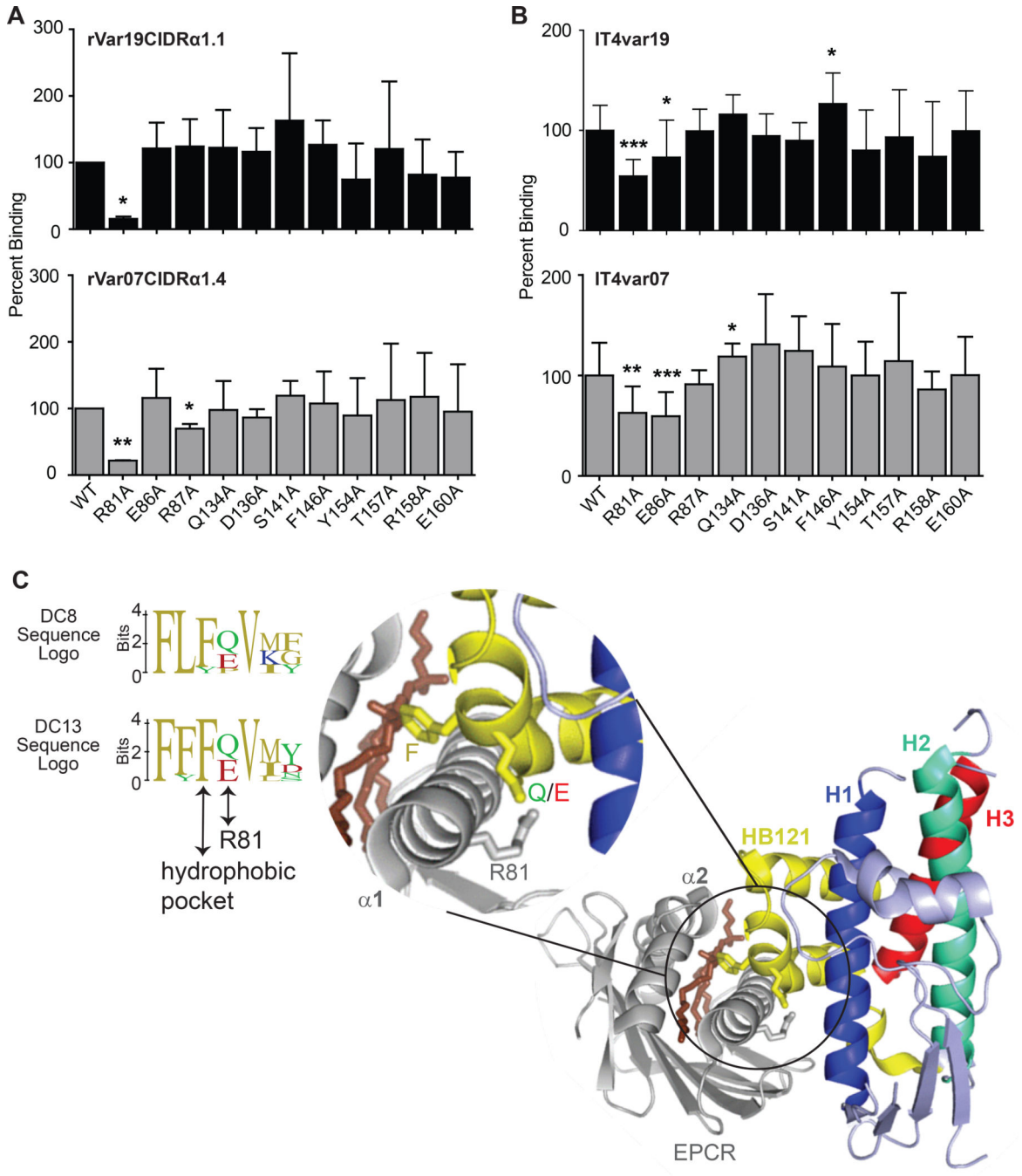

Fig. 5. R81 in EPCR plays a pivotal role in *P. falciparum* recognition

A. Binding of DC8 Var19CIDRα1.1 (black bars) and DC13 Var07CIDRα1.4 (grey bars) recombinant proteins to wild-type and mutant EPCR variants (mean and error, n = 2 – 4 independent experiments).

B. Binding of *P. falciparum*-IEs expressing IT4var19 (black bars) and IT4var07 (grey bars) to wild-type and mutant EPCR variants (mean and error, n = 2 – 3 independent experiments).

C. Ribbon diagram of the solved Var07CIDRα1.4-EPCR co-crystal structure (PDB 4V3E) from Lau et al. (Lau *et al.*, 2015) and sequence logo showing conservation of key CIDRα1-EPCR contact residues in DC8 and DC13 domains. The inset shows a close-up view of the conserved phenylalanine residue that inserts into the EPCR lipid binding groove and the adjacent R81-Q/E interaction; EPCR (grey), the bound phospholipid (brown). The H1, H2, and H3 helices forming the conserved helical bundle in Var07CIDRα1.4 and HB121 homology block are indicated.

In (A) and (B), binding is normalized for the surface expression levels of EPCR variants compared to wild-type EPCR using mAbs 252 and 1500 from Figure 4. A one-sample t test was used to detect significance in binding between EPCR mutants and wild type EPCR.

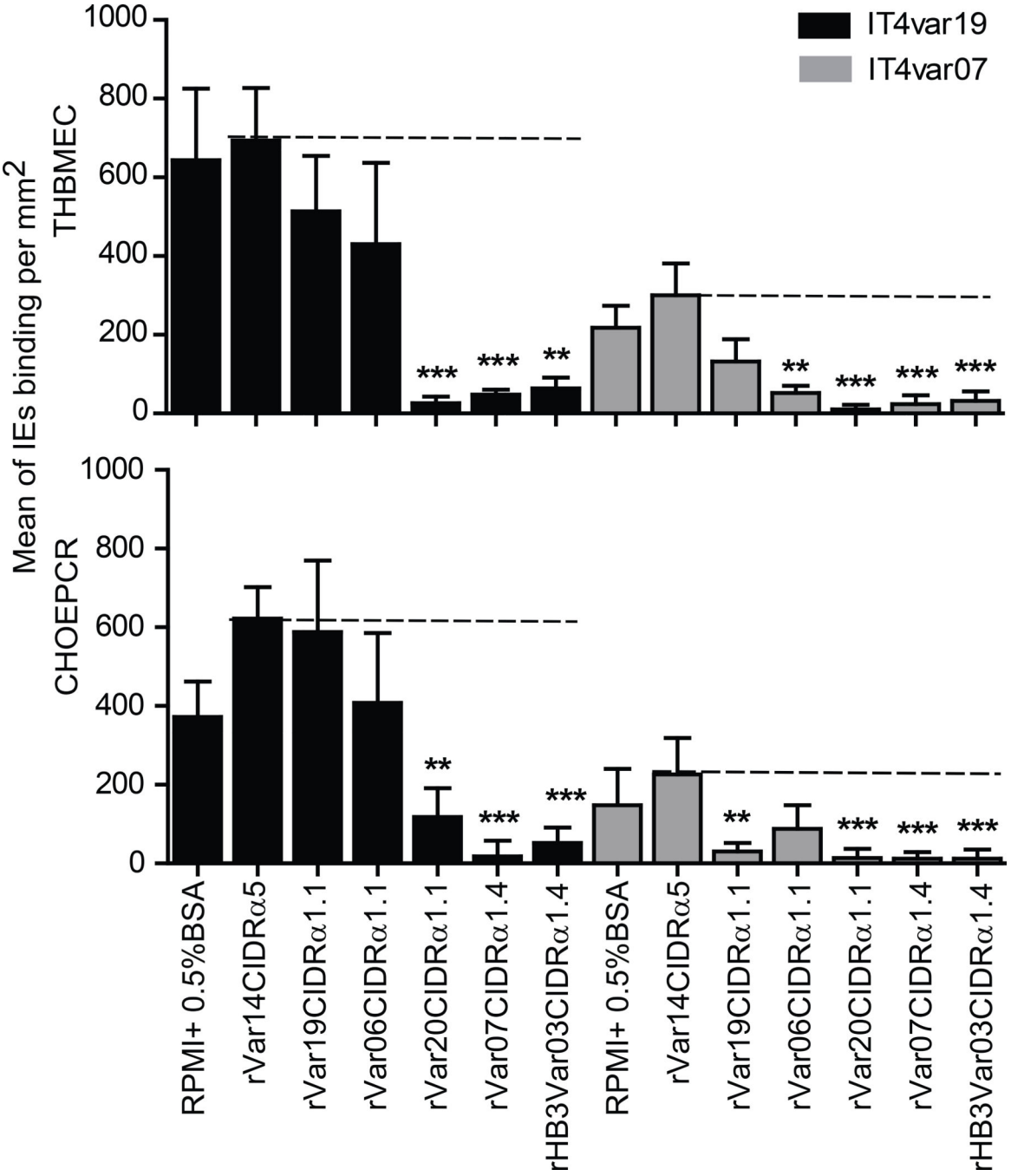

Fig. 6.

CIDRα1.1 and CIDRα1.4 domains cross-inhibit parasite adhesion to EPCR-expressing cells. Parasite lines expressing IT4var19 (DC8 CIDRα1.1, black bars) or IT4var07 (DC13 CIDRα1.4, grey bars) were compared for binding to THBMEC or CHO-EPCR cells. Prior to the IE binding assay, cell monolayers were pre-incubated in the presence or absence of recombinant CIDR domains. Data represents mean and error (n = 2 independent experiments). Results were analyzed by Kruskal-Wallis one-way ANOVA test.

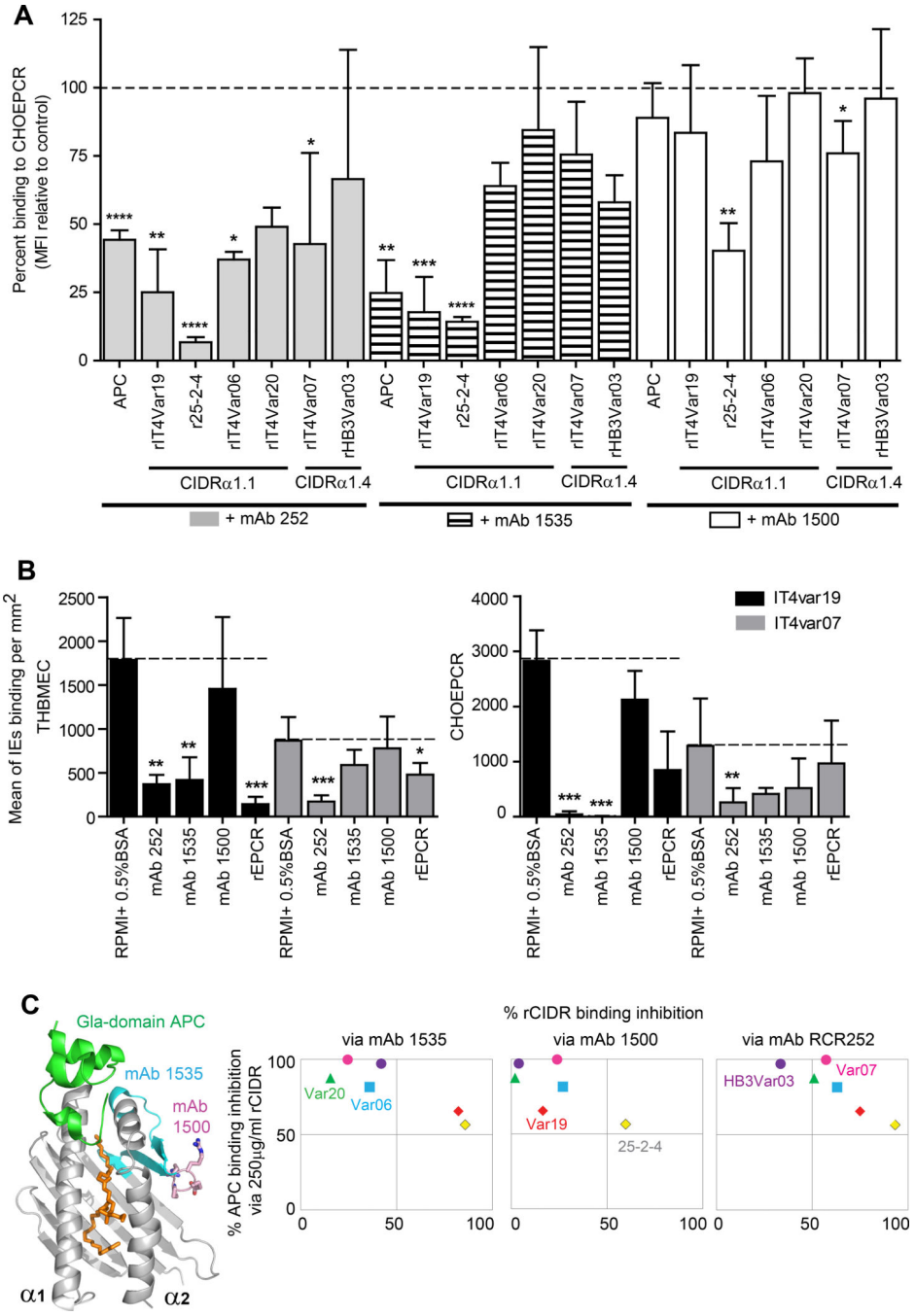

Fig. 7. Differential inhibition of CIDRα1 domains by anti-EPCR mAbs

A. Inhibition of APC or CIDRα1 domains binding to CHO-EPCR by anti-EPCR mAbs (252, 1535, and 1500) was analyzed by flow cytometry. The dotted line indicates the 100% binding level in the absence of mAbs. Data represents mean and error (n = 2 – 4 independent experiments). Results were analyzed by one-sample t test.

B. Inhibition of parasite lines expressing IT4var19 (DC8 CIDRα1.1, black bars) and IT4var07 (DC13 CIDRα1.4, grey bars) binding to THBMEC or CHO-EPCR cells by anti-

EPCR antibodies or soluble recombinant EPCR (mean and error, n = 2 – 3 independent experiments). Results were analyzed by Kruskal-Wallis one-way ANOVA test

C. The ability of anti-EPCR mAbs to inhibit CIDRα1 binding to CHO-EPCR cells is plotted against the percentage of APC blockade by those CIDRα1 domains from Fig. 3. The regions recognized by APC-blocking antibody 1535 (blue) and non-APC blocking antibody 1500 (pink) (Liaw *et al.*, 2001) are shown on the solved EPCR-APC co-crystal (PDB 1L8J) (Oganesyan *et al.*, 2002). In the ribbon schematic, EPCR is grey, the Gla-domain of APC is green, and the phospholipid is orange.